Applied Microbiology and Biotechnology (2021) 105:5895–5904
https://doi.org/10.1007/s00253-021-11440-6

APPLIED GENETICS AND MOLECULAR BIOTECHNOLOGY

Improving the functionality of surface-engineered yeast cells by altering the cell wall morphology of the host strain

Kentaro Inokuma[1] · Yuki Kitada[1] · Takahiro Bamba[1] · Yuma Kobayashi[1] · Takahiro Yukawa[1] · Riaan den Haan[2] · Willem Heber van Zyl[3] · Akihiko Kondo[1,4,5] · Tomohisa Hasunuma[1,4]

Received: 22 April 2021 / Revised: 21 June 2021 / Accepted: 3 July 2021 / Published online: 17 July 2021

Abstract

The expression of functional proteins on the cell surface using glycosylphosphatidylinositol (GPI)-anchoring technology is a promising approach for constructing yeast cells with special functions. The functionality of surface-engineered yeast strains strongly depends on the amount of functional proteins displayed on their cell surface. On the other hand, since the yeast cell wall space is finite, heterologous protein carrying capacity of the cell wall is limited. Here, we report the effect of *CCW12* and *CCW14* knockout, which encode major nonenzymatic GPI-anchored cell wall proteins (GPI-CWPs) involved in the cell wall organization, on the heterologous protein carrying capacity of yeast cell wall. *Aspergillus aculeatus* β-glucosidase (BGL) was used as a reporter to evaluate the protein carrying capacity in *Saccharomyces cerevisiae*. No significant difference in the amount of cell wall–associated BGL and cell-surface BGL activity was observed between *CCW12* and *CCW14* knockout strains and their control strain. In contrast, in the *CCW12* and *CCW14* co-knockout strains, the amount of cell wall–associated BGL and its activity were approximately 1.4-fold higher than those of the control strain and *CCW12* or *CCW14* knockout strains. Electron microscopic observation revealed that the total cell wall thickness of the *CCW12* and *CCW14* co-knockout strains was increased compared to the parental strain, suggesting a potential increase in heterologous protein carrying capacity of the cell wall. These results indicate that the *CCW12* and *CCW14* co-knockout strains are a promising host for the construction of highly functional recombinant yeast strains using cell-surface display technology.

Key points

- *CCW12 and/or CCW14 of a BGL-displaying S. cerevisiae strain were knocked out.*
- *CCW12 and CCW14 co-disruption improved the display efficiency of BGL.*
- *The thickness of the yeast cell wall was increased upon CCW12 and CCW14 knockout.*

Keywords *Saccharomyces cerevisiae* · Yeast surface display · Glycosylphosphatidylinositol-anchored cell wall protein · cell wall morphology

✉ Tomohisa Hasunuma
hasunuma@port.kobe-u.ac.jp

[1] Graduate School of Science, Technology and Innovation, Kobe University, 1-1 Rokkodai-cho, Nada-ku, Kobe 657-8501, Japan

[2] Department of Biotechnology, University of the Western Cape, Bellville 7530, South Africa

[3] Department of Microbiology, Stellenbosch University, Private Bag X1, Matieland 7602, South Africa

[4] Engineering Biology Research Center, Kobe University, 1-1 Rokkodai-cho, Nada-ku, Kobe 657-8501, Japan

[5] Biomass Engineering Program, RIKEN, 1-7-22 Suehiro-cho, Tsurumi-ku, Yokohama, Kanagawa 230-0045, Japan

Introduction

The expression of functional proteins on the cell surface is a promising approach to add special functions to microbial cells and yeast *Saccharomyces cerevisiae* is the most frequently used host microorganism for this approach. Yeast cell-surface display technology essentially relies on the expression of a target protein in the cell wall through linkage with a genetically fused anchoring protein, typically a glycosylphosphatidylinositol (GPI)-anchored cell wall protein (GPI-CWP). Cell-surface-engineered yeast strains constructed using this technology

can be used for a wide range of applications, such as the engineering and screening of enzymes, antibodies, or peptides (Angelini et al. 2015; Grzeschik et al. 2017; Li et al. 2007), biocontrol agents (Zhao et al. 2020), and the production of whole cell catalysts for bioconversion (Liu et al. 2016; Inokuma et al. 2018), biodegradation (Shibasaki et al. 2009), and biosensing (Shibasaki et al. 2001; Wang et al. 2013). Furthermore, the applications of antigen-displaying cells as vaccines against influenza viruses were recently reported (Lei et al. 2016; Lei et al. 2020).

The functionality of yeast cells strongly depends on the amount of proteins displayed on their cell surface and many studies to efficiently immobilize heterologous proteins to cell surface have been reported over the years. A typical method is the overexpression of target genes using constitutive promoters with high strength and/or adding extra copies of gene cassettes (Yamakawa et al. 2012; Inokuma et al. 2015). Optimization of the gene cassette introduced into yeast is another promising method for improving the efficiency of yeast surface display. We have successfully enhanced the cell-surface β-glucosidase (BGL) and endoglucanase (EG) activity by 17- and 108-fold, respectively, by optimizing the gene cassette components (combination of promoter, GPI anchoring region, and secretion signal sequences) (Inokuma et al. 2014; Inokuma et al. 2016).

Another approach to improve the display efficiency of heterologous proteins is the genetic engineering of the host yeast strain. Since the extracellular transport mechanism of GPI-attached proteins is fundamentally the same as that of secretory proteins and surface display data correlate well with secretion data (Shusta et al. 1999), the yeast cell-surface display technology can be used to explore targets to improve protein secretion efficiency. Hence, many of the reported engineering targets for improving surface display efficiency are involved in the protein secretion pathway. In addition, there are some reports on improving the surface display efficiency via engineering genes encoding yeast cell wall proteins. Wentz and Shusta (2007) performed a genome-wide screening of engineering targets that improve the display of heterologous proteins and found that overexpression of some genes encoding nonenzymatic GPI-CWPs (Ccw12p, Cwp2p, and Sed1p) promotes the display of a single-chain T-cell receptor. Bamba et al. (2018) reported approximately 20% increase in the amount of the cell wall–associated BGL by disruption of the *SED1* gene. These reports suggested that nonenzymatic GPI-CWPs are promising targets to improve surface display efficiency. However, there is limited knowledge about the engineering effect of cell wall proteins, especially on the heterologous protein carrying capacity of the yeast cell wall.

In the present study, we focused on Ccw12p and Ccw14p, major nonenzymatic GPI-CWPs involved in cell wall organization in *S. cerevisiae* (https://www.yeastgenome.org/go/GO:0031505), and investigated the effect of disrupting the *CCW12* and *CCW14* on the heterologous protein carrying capacity of the cell wall using *Aspergillus aculeatus* BGL1 as the reporter protein. Ccw12p is a heavily glycosylated GPI-CWP of 133 amino acids concentrated at sites of active cell wall synthesis such as the future bud site, the septum, and the lateral walls of enlarging daughter cells, and has a major role in the cell wall integrity in *S. cerevisiae* (Ragni et al. 2007; Ragni et al. 2011). Ccw14p is a GPI-CWP of 238 amino acids localized to the inner cell wall (Moukadiri et al. 1997), and involved in cell wall stability (Lesage and Bussey 2006) and biofilm formation (Moreno-García et al. 2018). Ccw12p and Ccw14p have been reported to be related to yeast cell wall chitin (Klis 1994; Moukadiri et al. 1997), which plays an important role in the mechanical strength of the cell wall (Arroyo et al. 2016). First, *CCW12* and *CCW14* of a BGL-displaying *S. cerevisiae* strain were knocked out individually or simultaneously using a CRISPR/Cas9-mediated gene knockout method. Then, cell-surface BGL activity and the amount of cell wall–associated BGL in the constructed strains were compared to those of the parental strain. Finally, the effect of the *CCW12* and *CCW14f* knockout on the cell wall morphology of the BGL-displaying strains was investigated using transmission electron microscopy.

Materials and methods

Strains and media

Escherichia coli strain DH5α (Toyobo, Osaka, Japan) was used for the construction and propagation of all plasmids as described previously (Inokuma et al. 2016). All yeast strains used in this study were derived from the haploid strain *S. cerevisiae* BY4741 (Life Technologies, Carlsbad, CA, USA). Genetic properties of the *S. cerevisiae* strains used in this study are summarized in Table 1.

S. cerevisiae transformants were screened and cultivated as previously described (Inokuma et al. 2016). The culture broth was sampled every 24 h, and yeast cells were harvested via centrifugation at 1000 × *g* for 5 min, washed twice with distilled water, and centrifuged again at 1000 × *g* for 5 min. The wet cell weight of the washed yeast cells was determined by weighing the cell pellet and the dry cell weight of a yeast cell was determined (approximately 0.15 × its wet cell weight (Inokuma et al. 2014)). Cell pellets were used for enzyme assays and ethanol fermentation.

Table 1 Characteristics of yeast strains and plasmids used in this study

Yeast strains and plasmids	Relevant genotype	Source
S. cerevisiae		
BY4741	*MAT**a** his3Δ1 leu2Δ0 met15Δ0 ura3Δ0*	Life Technologies
BY-BG-SSS	BY4741/pIBG-SSS [$SED1_P$–$SED1_{SP}$–*A. aculeatus BGL1*–$SED1_A$–$SAG1_T$, *leu2Δ0 met15Δ0 ura3Δ0*]	Inokuma et al. (2016)
BY-BG-SSSD	BY4741/pIBG-SSSD [$SED1_P$–$SED1_{SP}$–*A. aculeatus BGL1*–$SED1_A$–$DIT1_T$, *leu2Δ0 met15Δ0 ura3Δ0*]	This study
ccw12-BGSD	BY-BG-SSSD *CCW12Δ* [$SED1_P$–$SED1_{SP}$–*A. aculeatus BGL1*–$SED1_A$–$DIT1_T$, *leu2Δ0 met15Δ0 ura3Δ0 ccw12Δ*]	This study
ccw14-BGSD	BY-BG-SSSD *CCW14Δ* [$SED1_P$–$SED1_{SP}$–*A. aculeatus BGL1*–$SED1_A$–$DIT1_T$, *leu2Δ0 met15Δ0 ura3Δ0 ccw14Δ*]	This study
ccw12/ccw14-BGSD	BY-BG-SSSD *CCW12ΔCCW14Δ* [$SED1_P$–$SED1_{SP}$–*A. aculeatus BGL1*–$SED1_A$–$DIT1_T$, *leu2Δ0 met15Δ0 ura3Δ0 ccw12Δ ccw14Δ*]	This study
BY-EG-SSSD	BY4741/pIEG-SSSD [$SED1_P$–$SED1_{SP}$– *T. reesei EGII*–$SED1_A$–$DIT1_T$, *leu2Δ0 met15Δ0 ura3Δ0*]	This study
ccw12/ccw14-EGSD	BY-EG-SSSD *CCW12ΔCCW14Δ* [$SED1_P$–$SED1_{SP}$– *T. reesei EGII*–$SED1_A$–$DIT1_T$, *leu2Δ0 met15Δ0 ura3Δ0 ccw12Δ ccw14Δ*]	This study
BY-BG-SSAD	BY4741/pIBG-SSAD [$SED1_P$–$SED1_{SP}$–*A. aculeatus BGL1*–$SAG1_A$–$DIT1_T$, *leu2Δ0 met15Δ0 ura3Δ0*]	This study
ccw12/ccw14-BGAD	BY4741/pIBG-SSAD *CCW12ΔCCW14Δ* [$SED1_P$–$SED1_{SP}$–*A. aculeatus BGL1*–$SAG1_A$ –$DIT1_T$, *leu2Δ0 met15Δ0 ura3Δ0 ccw12Δ ccw14Δ*]	This study
Plasmids		
pIBG-SSS	*HIS3* $SED1_P$–$SED1_{SP}$–*A. aculeatus BGL1*–$SED1_A$–$SAG1_T$	Inokuma et al. (2016)
pIBG-SSSD	*HIS3* $SED1_P$–$SED1_{SP}$–*A. aculeatus BGL1*–$SED1_A$–$DIT1_T$	This study
pIEG-SSS	*HIS3* $SED1_P$–$SED1_{SP}$–*T. reesei EGII*–$SED1_A$–$SAG1_T$	Inokuma et al. (2016)
pIEG-SSSD	*HIS3* $SED1_P$–$SED1_{SP}$–*T. reesei EGII*–$SED1_A$–$DIT1_T$	This study
pIBG13	*HIS3* $TDH3_P$–*A. aculeatus BGL1*–$SAG1_A$–$SAG1_T$	Katahira et al. (2006)
pIBG-SSAD	*HIS3* $SED1_P$–$SED1_{SP}$–*A. aculeatus BGL1*–$SAG1_A$–$DIT1_T$	This study
pGK415	CEN-ARS *LEU2* $PGK1_P$–$PGK1_T$	Ishii et al. (2009)
Cas9_Base	*K. marxianus ARS7*, *K. marxianus* CEN D, *kanMX* $PDC1_P$–*Cas9*–$TDH3_T$	Nambu-Nishida et al. (2017)
pCL-Cas9	CEN-ARS *LEU2* $TEF1_P$–$SV40_{NLS}$–*Cas9*–$SV40_{NLS}$–$CYC1_T$	This study
pGK426	2μ ori *URA3* $PGK1_P$–$PGK1_T$	Ishii et al. (2009)
pSUP4t	2μ ori *URA3* $SUP4_T$	This study
p2gRNA-CCW12	2μ ori *URA3* $SNR52_P$–gRNA for *CCW12*–$SUP4_T$	This study
p2gRNA- CCW14	2μ ori *URA3* $SNR52_P$–gRNA for *CCW14*–$SUP4_T$	This study
p2gRNA-CCW12/CCW14	2μ ori *URA3* $SNR52_P$–gRNA for *CCW12*–$SUP4_T$ $SNR52_P$–gRNA for *CCW14*–$SUP4_T$	This study

A. aculeatus, *Aspergillus aculeatus*; *T. reesei*, *Trichoderma reesei*; *K. marxianus*, *Kluyveromyces marxianus*; *P* promoter, *SP* secretion signal peptide sequence, *A* anchoring region, *T* terminator, *NLS* nuclear localization signal

Plasmid construction and yeast transformation

The plasmids and primers used in this study are listed in Table 1 and Supplemental Table S1, respectively. Details on the construction of plasmids and yeast transformation are provided as Supplemental Text S1. All plasmids used in this study were transformed into *S. cerevisiae* using the lithium acetate method (Chen et al. 1992).

CRISPR/Cas9-mediated gene knockout with a double-stranded oligonucleotide

CCW12 and/or *CCW14* knockout strains were constructed using the CRISPR/Cas9-mediated gene knockout method (Jakočiūnas et al. 2015). The double-stranded oligo-nucleotides (dsOrigos) used in this study are listed in Supplemental Table S2. Specific guide RNAs (gRNAs) targeting *CCW12* and *CCW14* were designed using CHOPCHOP v3 (http://chopchop.cbu.uib.no). gRNAs without 100% identity to other loci in the chromosomal DNA of the *S. cerevisiae* S288c strain were selected.

Briefly, the pCL-Cas9 plasmid was transformed into BY-BG-SSSD, BY-EG-SSSD, and BY-BG-SSAD to express Cas9. Next, appropriate gRNA expression plasmids were transformed into the Cas9-expressing strain with 1 nmol of corresponding dsOrigos, and the transformants were cultivated on selective agar plates for 72 h to knock out *CCW12* and/or *CCW14*. Base editing of the targeted loci was validated via Sanger sequencing. Finally, the *CCW12* and/or *CCW14* knockout strains were cultivated in the yeast extract peptone dextrose (YPD) medium for 24 h to eliminate Cas9 and gRNA expression plasmids. The plasmid elimination was verified by screening on agar plates with selective pressure for each plasmid. The strains in which both plasmids were eliminated were used for subsequent experiments as *CCW12* and/or *CCW14* knockout strains.

Enzyme assays

BGL and EG activities of washed yeast cell pellets were evaluated as described previously (Inokuma et al. 2016). Briefly, BGL activity was assayed at pH 5.0 and 30 °C with 2 mM *p*-nitrophenyl-β-D-glucopyranoside (*p*NPG) as substrate. One unit of BGL activity was defined as the amount of enzyme required to liberate 1 μmol of *p*-nitrophenol per min. EG activity for water-insoluble cellulose was assayed at pH 5.0 and 38 °C using water-insoluble AZCL-HE-Cellulose (Cellazyme C tablets; Megazyme, Bray, Ireland) as the substrate.

Transcript quantification of *BGL1* using real-time PCR

The transcript levels of *BGL1* were quantified using real-time PCR as described previously (Liu et al. 2017). The primers used are listed in Supplemental Table S1. Gene expression levels of target genes were normalized to those of the housekeeping β-tubulin gene (*TUB2*).

Relative quantitative analysis of cell wall–associated BGL

The identification and relative quantification of BGL in the yeast cell wall were performed based on precise mass measurements of tryptic peptides from the reporter protein using nanoscale ultra-pressure liquid chromatography-electrospray ionization quadrupole time-of-flight tandem mass spectrometry (nano-UPLC-MS^E) and ProteinLynx Global SERVER v3.0 (Waters Corporation, Milford, MA, USA), as described previously (Bamba et al. 2018). A minor modification was the use of an AQC M-Class HSS T3 Column (75 μm × 150 mm; particle size, 1.8 μm; Waters Corporation) as the analytical column.

Electron microscopy analysis

Rapid freezing and freeze-substitution of washed cell pellets were carried out as described previously (Inokuma et al. 2020). The substituted samples were transferred to −20 °C for 3 h and then warmed to 4 °C over 4 h. Next, they were dehydrated in ethanol 3 times at room temperature for 30 min each and continuously dehydrated with ethanol overnight. Infiltration was performed with propylene oxide (PO) and resin (Quetol-651; Nisshin EM Co., Tokyo Japan) at room temperature [100% PO for 30 min; 100% PO for 30 min; PO:resin 50:50 for 3 h; 100% resin overnight]. The resins were then polymerized at 60 °C for 48 h and cut into ultrathin sections of 70 nm thick using an ultramicrotome (Ultracut CUT; Leica, Vienna, Austria). The ultrathin sections were placed on copper grids, stained with 2% uranyl acetate for 15 min and lead stain solution (Sigma-Aldrich, St. Louis, MO, USA) for 3 min at room temperature. They were observed using a transmission electron microscope (JEM-1400Plus; JOEL Ltd., Tokyo Japan) at an acceleration voltage of 100 kV. Digital images (3296 × 2472 pixels) were taken with a CCD camera (EM-14830RUBY2; JOEL Ltd.).

Sensitivity of yeast cells to chitin-binding reagents

Yeast cells were grown in the YPD medium to exponential phase. Cells were harvested and resuspended in sterile water at an OD_{600} of 1 (Approximately 10^8 cells/mL). Serial 10-fold dilutions thereof were prepared and spotted (5 μL) onto YPD plates alone or containing 20 μg/mL Calcofluor white (CFW) or 30 μg/mL Congo red (CR). Growth on plates was evaluated after 2 days of incubation at 30 °C.

Statistical analysis

Student's *t*-tests with Bonferroni correction were used to compare groups of values. Difference with confidence level of 95% ($p < 0.05$) was considered statistically significant.

Results

Construction of BGL-displaying *S. cerevisiae* strains

To evaluate the effect of *CCW12* and *CCW14* disruptions on the surface display efficiency of heterologous proteins, we

used *A. aculeatus* BGL1 as the reporter protein as it has been reported that this enzyme shows a good proportional relationship between its activity and abundance in the cell wall (Bamba et al. 2018; Inokuma et al. 2020). *S. cerevisiae* Sed1p, which is a stress-induced nonenzymatic GPI-CWP, was used as the anchoring domain for the cell-surface display because this protein has an excellent effect on the display of heterologous proteins including BGL1 (Inokuma et al. 2014; Inokuma et al. 2016). BGL1 was genetically fused Sed1p and the gene cassette for the expression of this fusion protein was integrated into the *HIS3* locus of the chromosomal DNA of *S. cerevisiae* BY4741 via homologous recombination. We adopted the terminator sequence derived from *S. cerevisiae DIT1* (Ito et al. 2016) to the BGL-displaying cassette because the *DIT1* terminator exhibited high performance in the surface display of BGL1 compared with the conventional *SAG1* terminator (Supplemental Fig. S1). *CCW12* and *CCW14* of the constructed BGL-displaying strains (BY-BG-SSSD) were then knocked out individually or simultaneously using the CRISPR/Cas9-mediated gene knockout method (Jakočiūnas et al. 2015) as described in the Materials and methods. Data obtained via Sanger sequencing of targeted loci from 4 colonies of each transformation showed stop codons in all the genomic contexts according to dsOligo template designs (Fig. 1). The constructed strains, ccw12-BGSD (*CCW12Δ*), ccw14-BGSD (*CCW14Δ*), and ccw12/ccw14-BGSD (*CCW12ΔCCW14Δ*), were used in subsequent experiments with BY-BG-SSSD as the reference strain. The detailed information of these strains is shown in Table 1.

Enzyme activity and relative quantity of cell wall–associated BGL1

The BGL-displaying strains were cultivated at 30 °C for 96 h and cell-surface BGL activity was evaluated every 24 h. BGL activity of these strains reached a plateau after 48 h of cultivation (Fig. 2a). No significant difference in the cell-surface BGL activity was observed between the control strain (BY-BG-SSSD) and *CCW12* or *CCW14* knockout strains (ccw12-BGSD and ccw14-BGSD). In contrast, in the *CCW12* and *CCW14* co-knockout strains (ccw12/ccw14-BGSD), the cell-surface BGL activity was significantly higher than that of the control strain (BY-BG-SSSD) and the control strain (BY-BG-SSSD) and *CCW12* or *CCW14* knockout strains (ccw12-BGSD and ccw14-BGSD). The BGL activity of the ccw12/ccw14-BGSD strain reached 1250 ± 11 U/g dry cells after 48 h, which was approximately 1.4-fold higher than that of the control strain (826 ± 23 U/g dry cells). During cultivation, no significant growth defects were observed due to *CCW12* and *CCW14* knockout (Fig. 2b).

We also investigated the expression levels of *A. aculeatus BGL1* in these strains using real-time PCR. No significant difference was observed in the expression levels of the gene in these strains after 48 h of cultivation (Fig. 2c).

Subsequently, the relative quantification of cell wall–associated BGL in these strains was performed using nano-UPLC-MS^{E}. The amount of cell wall–associated BGL per unit dry cell weight of ccw12/ccw14-BGSD was approximately 1.4-fold higher than that of the control strain, while that of ccw12-BGSD and ccw14-BGSD did not show any significant change (Fig. 2d). This result correlated well with cell-surface BGL activity of these strains (Fig. 2a), suggesting that the increased cell-surface BGL activity in ccw12/ccw14-BGSD was due to the increase in the amount of cell wall–associated BGL.

Electron microscopic observation of BGL-displaying cells

In order to understand the effect of *CCW12* and *CCW14* disruption better, cell wall morphology of the BGL-displaying yeast strains was observed under a transmission electron microscope (Fig. 3). Compared to the control strain (BY-BG-SSSD, Fig. 3a), the cell wall of the ccw12-BGSD strain appeared noticeably darker, indicating an increased electron density (Fig. 3b). Although there was no significant change in total cell wall thickness, the proportion of the outer mannan layer was significantly increased. In contrast, in the ccw14-

Fig. 1 Sequence alignments of *CCW12* and *CCW14* compared to their respective dsOligos. The sense strands of the target sites are shown. The green sequences of the wild-type reference sequence denote the protospacer adjacent motif (PAM) sites. The red sequences indicate stop codons replacing the PAM sites. Sequences present in the gRNAs are underlined

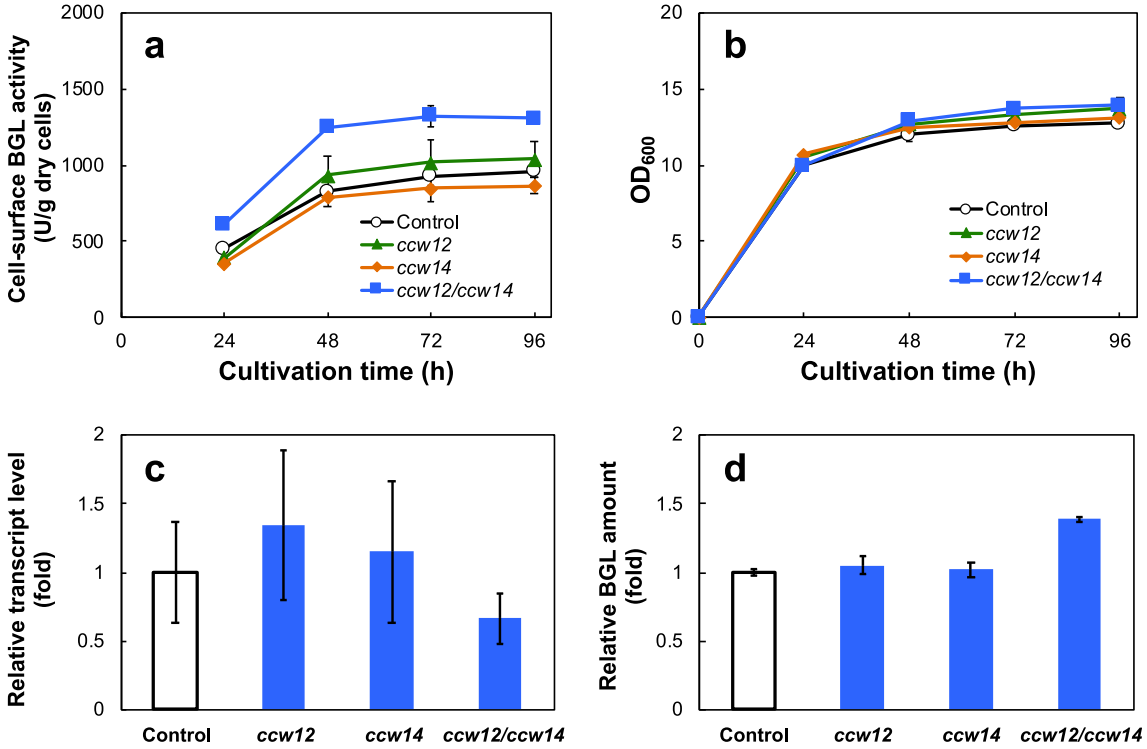

Fig. 2 Effects of *CCW12* and/or *CCW14* knockout on BGL-displaying yeast. **a** Time-course of cell-surface BGL activities. **b** Cell growth of BGL-displaying yeasts. **c** Comparison of transcript levels of BGL1-encoding genes after cultivation in YPD medium for 48 h. The relative transcript level of each gene is shown as a fold-change in mRNA levels relative to the average level detected in the control strain (BY-BG-SSSD). **d** Relative quantification of BGL1 in the cell walls by nano-UPLC-MS^{E}. The amount of BGL1 was normalized to the dry cell weight of each strain. Data are presented as the means ± standard deviation (n = 3)

BGSD strain, the inner glucan layer was less dense and brush-like fibers in the outer mannan layer were reduced and disturbed (Fig. 3c). In the ccw12/ccw14-BGSD strain, the density of the cell wall was intermediate between ccw12-BGSD and ccw14-BGSD, while the total cell wall thickness was noticeably increased (Fig. 3d; 200–230 nm) compared to the other three strains (Fig. 3a, b, and c; 140–170 nm).

Discussion

The *CCW12* and *CCW14* genes encode major nonenzymatic GPI-CWPs involved in cell wall organization in *S. cerevisiae* (https://www.yeastgenome.org/go/GO:0031505). In this study, we investigated the effect of *CCW12* and *CCW14* knockout on the surface display efficiency of heterologous proteins in yeast. No significant difference in the amount of cell wall–associated BGL per cell weight was observed between strains in which *CCW12* or *CCW14* was knocked out and their control strain. In contrast, in the *CCW12* and *CCW14* co-knockout strains, the amount of cell wall–associated BGL was approximately 1.4-fold higher than that of the control strain and *CCW12* or *CCW14* knockout strains (Fig. 2d). With the increase of the cell wall–associated BGL, the *CCW12* and *CCW14* co-knockout strains showed improved cell-surface BGL activity (Fig. 2a) compared to the control strain and *CCW12* or *CCW14* knockout strains, while no significant growth defects were observed due to the knockout of these genes (Fig. 2b).

We also conducted electron microscopy analysis of the ultrathin sections of BGL-displaying strains and revealed their morphological differences (Fig. 3). ccw12-BGSD and ccw14-BGSD strains showed contrasting morphological abnormalities in the cell wall; i.e., the cell wall density was higher in the ccw12-BGSD strain and lower in the ccw14-BGSD strain than that in their parental strain (BY-BG-SSSD). In contrast, *CCW12* and *CCW14* co-disruption had an unexpected morphological phenotype. The total cell wall thickness of the ccw12/ccw14-BGSD strain was significantly increased (Fig. 3d; 200–230 nm) compared to the other three strains (Fig. 3a, b, and c; 140–170 nm). In the GPI anchoring technology, GPI-attached heterologous proteins are immobilized in the yeast cell wall through covalent linkage to a β-(1 to 6) glucan (Lu et al. 1994). We previously reported that GPI-attached heterologous proteins in the cell wall are sterically immobilized in the cell wall space (Inokuma et al. 2020). The observations shown in Fig. 3 suggest that the increased BGL amount in the ccw12/ccw14-BGSD strain was due to an increase in the protein capacity of the cell wall with the expansion of the cell wall space.

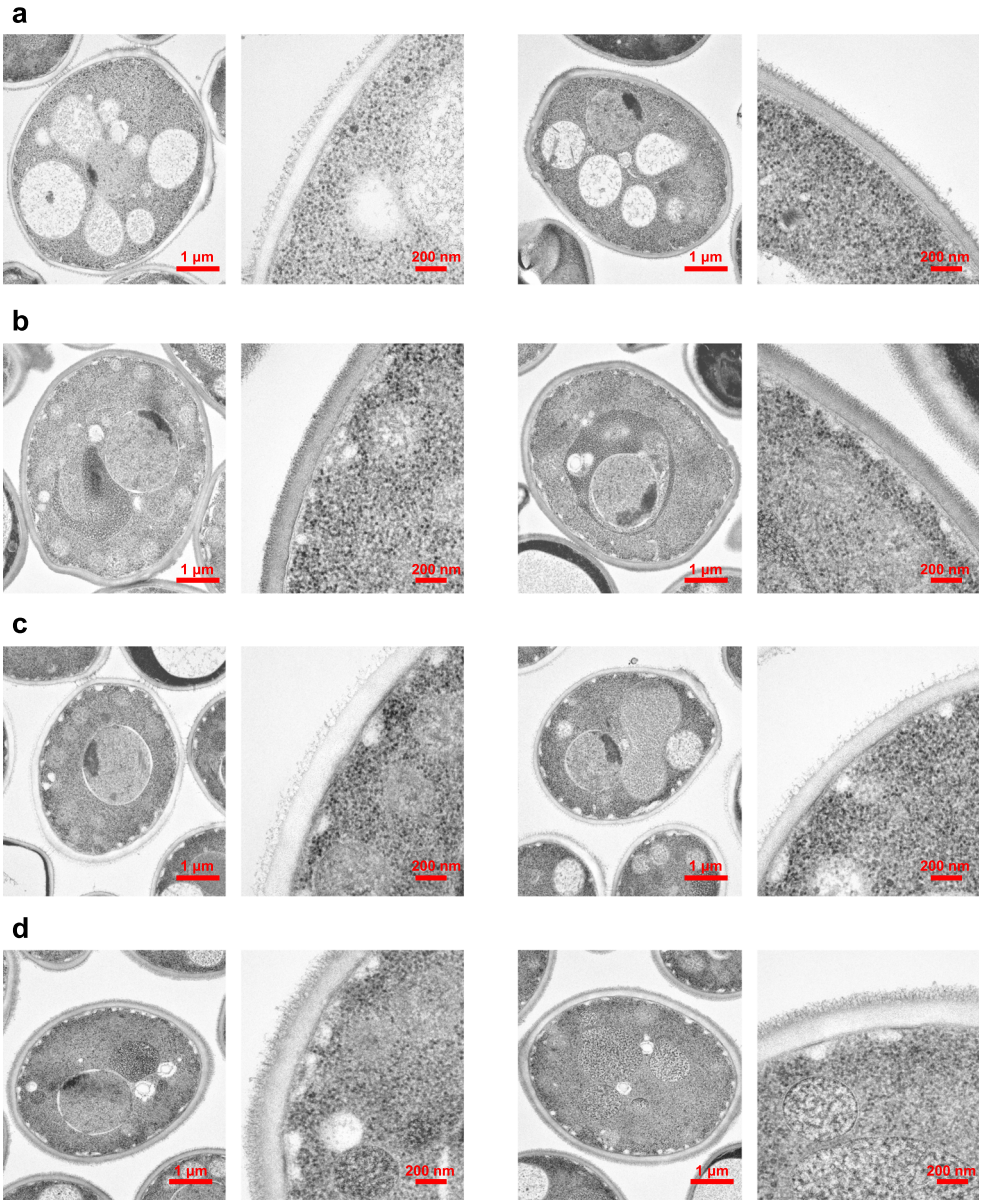

Fig. 3 Electron micrographs of ultrathin sections of **a** BY-BG-SSSD, **b** ccw12-BGSD, **c** ccw14-BGSD, and **d** ccw12/14-BGSD cells

The molecular mechanism underlying morphological changes in the cell wall and increased heterologous protein capacity in the *CCW12* and *CCW14* co-knockout strains is still unclear. It has been reported that yeast cells lacking *CCW12* show increased chitin content and hypersensitivity to chitin-binding reagents CFW and CR (Klis 1994). Also, deletion of *CCW14* leads to increased sensitivity to these reagents (Moukadiri et al. 1997). Chitin is one of the main components of the yeast cell wall. Chitin and glucan are covalently linked to form a network that is responsible for the mechanical strength of the cell wall (Arroyo et al. 2016). Severe chitin abnormality caused by the *CCW12* and *CCW14* co-disruption might have reduced the mechanical strength of the chitin-glucan network and increased the flexibility of the cell wall of the ccw12/ccw14-BGSD strain, increasing the cell wall thickness. We performed sensitivity assays to CFW and CR for the BGL-displaying strains (Supplemental Fig. S2). The *CCW12* and *CCW14* co-knockout strains (ccw12/ccw14-BGSD) showed increased sensitivity to CFW and CR compared with the control strain (BY-BG-SSSD) and ccw12-BGSD and ccw14-BGSD strains. This result also supports the severe chitin abnormality in ccw12/ccw14-BGSD. In contrast, ccw12-BGSD and ccw14-BGSD strains were not sensitive to CFW and CR contrary to previous reports, which showed that the deletion of *CCW12* or *CCW14* in *S. cerevisiae* markedly increases sensitivity to these reagents (Moukadiri et al. 1997; Mrsa et al. 1999). One possible cause for the insensitivity of ccw12-BGSD and ccw14-BGSD to CFW and CR in the present study might be the use of Sed1p as the GPI anchoring domain for the cell-

surface display of BGL. Shankarnarayan et al. (2008) reported that the hypersensitivity of the *S. cecevisiae* ccw12 mutant to CFW and CR is partially suppressed by elevated *SED1* expression. Sed1p as the GPI anchoring domain might also have played a role in suppressing the CFW and CR sensitivities of these strains. Sensitivity assays to CFW and CR and the electron microscopic observation using the *CCW12* and *CCW14* co-knockout strains without BGL display may help to better understand the function of these GPI-CWPs.

To verify generality and applicability of the *CCW12* and *CCW14* co-disruption strategy, we constructed the BGL-displaying strains using C-terminal domain of α-agglutinin (Sag1p), which is one of the major GPI anchoring domains used in the surface display of heterologous proteins (van der Vaart et al. 1997), instead of Sed1p (BY-BG-SSAD, Table 1) and investigated the effect of *CCW12* and *CCW14* knockout on its cell surface activity of BGL1 (Supplemental Fig. S3). The *CCW12* and *CCW14* co-disruption resulted in an approximate 1.2-fold increase in the cell-surface BGL activity of this strain, suggesting that this strategy could be applied to cell-surface display technology with not only Sed1p, also other GPI-CWPs. We also constructed the yeast strains displaying *Trichod*erma *reesei* EGII using Sed1p as the GPI anchoring domain (BY-EG-SSSD, Table 1) and investigated the effect of *CCW12* and *CCW14* knockout on its hydrolytic activity for water-insoluble cellulose (Supplemental Fig. S4). In contrast to the BGL activity, the hydrolytic activity of the EG-displaying strains was not significantly increased by *CCW12* and *CCW14* co-disruption. The substrate of BGL1 (*p*NPG) is a small molecule that can penetrate the cell wall and access all cell wall–associated enzymes, whereas water-insoluble cellulose, the substrate of EGII, is a large molecule and can only access the enzymes exposed on the external surface of the cell wall (Inokuma et al. 2020). Since the surface area of the cell wall would remain largely unchanged by increasing its thickness, *CCW12* and *CCW14* co-disruption might not have contributed to the cellulolytic activity of EG. The generality and applicability of the *CCW12* and *CCW14* co-disruption strategy would need to be further investigated using other proteins as well.

The results demonstrated in this study indicated that combinatorial engineering of multiple genes involved in the cell wall organization could be a promising approach to improve yeast cell-surface display technology, while they also suggested the difficulty of predicting the phenotypes caused by combinatorial engineering. Further exploration of yeast strains suitable for the cell-surface display technology using this approach would require the construction of a yeast genomic library with combinatorial engineering of multiple cell wall–related genes. Recently, several methods for the construction of a comprehensive yeast genomic library applying the CRISPR system have been proposed (Jakočiūnas et al. 2015; Lian et al. 2019). These technologies may be useful for combinatorial engineering to screen promising host strains for the yeast cell-surface display.

In conclusion, we investigated the effect of *CCW12* and *CCW14* disruption on the surface display efficiency of heterologous proteins using *A. aculeatus* BGL1 as the model protein. We found that the amount of cell wall–associated BGL and its activity in the *CCW12* and *CCW14* co-knockout strain were approximately 1.4-fold higher than those of the parental strain. Electron microscopic observation revealed that the total cell wall thickness of the *CCW12* and *CCW14* co-knockout strains was increased compared to the parental strain, suggesting an increase in the heterologous protein carrying capacity of the cell wall. Although further research is needed to elucidate the molecular mechanism, results of this study indicated that the *CCW12* and *CCW14* co-knockout strains are a promising host for the construction of highly functional recombinant yeast strains using cell-surface display technology. For example, the use of this strain for the production of whole cell catalysts could potentially speed up bioconversion and biodegradation processes and improve the sensitivity of biosensing. Furthermore, in the applications of antigen-displaying cells as vaccines (Lei et al. 2016; Lei et al. 2020), by increasing the amount of antigenic protein per cell weight, it would be able to induce an effective antigen-specific immune response with lower vaccine doses.

Supplementary Information The online version contains supplementary material available at https://doi.org/10.1007/s00253-021-11440-6.

Code availability Not applicable.

Author contribution KI designed the research and wrote the manuscript. TB designed the experiments. KI, TB, Y Kitada, and Y Kobayashi, TY performed the experiments. RDH, WHVZ, AK, and TH revised the manuscript. AK and TH conceived and supervised the research. All authors read and approved the manuscript.

Funding This work was supported in part by Japan Society for the Promotion of Science (JSPS) KAKENHI Grant Number JP18K05554, and JSPS and National Research Foundation (NRF) of South Africa under the JSPS-NRF Joint Research Program (JSPS Grant Number JPJSBP120196503 and NRF Grant Number 118894).

Data availability All relevant data generated during this study are included in the article and its supplementary information file.

Declarations

Ethics approval Not applicable.

Consent to participate Not applicable.

Consent for publication The authors approved the manuscript submission to *Applied Microbiology and Biotechnology*.

Conflict of interest The authors declare no competing interests.

References

Angelini A, Chen TF, de Picciotto S, Yang NJ, Tzeng A, Santos MS, Van Deventer JA, Traxlmayr MW, Wittrup KD (2015) Protein engineering and selection using yeast surface display. Methods Mol Biol 1319:3–36. https://doi.org/10.1007/978-1-4939-2748-7_1

Arroyo J, Farkaš V, Sanz AB, Cabib E (2016) Strengthening the fungal cell wall through chitin-glucan cross-links: effects on morphogenesis and cell integrity. Cell Microbiol 18(9):1239–1250. https://doi.org/10.1111/cmi.12615

Bamba T, Inokuma K, Hasunuma T, Kondo A (2018) Enhanced cell-surface display of a heterologous protein using *SED1* anchoring system in *SED1*-disrupted *Saccharomyces cerevisiae* strain. J Biosci Bioeng 125(3):306–310. https://doi.org/10.1016/j.jbiosc.2017.09.013

Chen DC, Yang BC, Kuo TT (1992) One-step transformation of yeast in stationary phase. Curr Genet 21(1):83–84. https://doi.org/10.1007/BF00318659

Grzeschik J, Hinz SC, Könning D, Pirzer T, Becker S, Zielonka S, Kolmar H (2017) A simplified procedure for antibody engineering by yeast surface display: coupling display levels and target binding by ribosomal skipping. Biotechnol J 12(2). https://doi.org/10.1002/biot.201600454

Inokuma K, Hasunuma T, Kondo A (2014) Efficient yeast cell-surface display of exo- and endo-cellulase using the *SED1* anchoring region and its original promoter. Biotechnol Biofuels 7(1):8. https://doi.org/10.1186/1754-6834-7-8

Inokuma K, Yoshida T, Ishii J, Hasunuma T, Kondo A (2015) Efficient co-displaying and artificial ratio control of α-amylase and glucoamylase on the yeast cell surface by using combinations of different anchoring domains. Appl Microbiol Biotechnol 99(4):1655–1663. https://doi.org/10.1007/s00253-014-6250-1

Inokuma K, Bamba T, Ishii J, Ito Y, Hasunuma T, Kondo A (2016) Enhanced cell-surface display and secretory production of cellulolytic enzymes with *Saccharomyces cerevisiae* Sed1 signal peptide. Biotechnol Bioeng 113(11):2358–2366. https://doi.org/10.1002/bit.26008

Inokuma K, Hasunuma T, Kondo A (2018) Whole cell biocatalysts using enzymes displayed on yeast cell surface. In: Chang H (ed) Emerging Areas in Bioengineering. Wiley-VCH, New York, pp 81–92

Inokuma K, Kurono H, den Haan R, van Zyl WH, Hasunuma T, Kondo A (2020) Novel strategy for anchorage position control of GPI-attached proteins in the yeast cell wall using different GPI-anchoring domains. Metab Eng 57:110–117. https://doi.org/10.1016/j.ymben.2019.11.004

Ishii J, Izawa K, Matsumura S, Wakamura K, Tanino T, Tanaka T, Ogino C, Fukuda H, Kondo A (2009) A simple and immediate method for simultaneously evaluating expression level and plasmid maintenance in yeast. J Biochem 145(6):701–708. https://doi.org/10.1093/jb/mvp028

Ito Y, Kitagawa T, Yamanishi M, Katahira S, Izawa S, Irie K, Furutani-Seiki M, Matsuyama T (2016) Enhancement of protein production via the strong *DIT1* terminator and two RNA-binding proteins in *Saccharomyces cerevisiae*. Sci Rep 6:36997. https://doi.org/10.1038/srep36997

Jakočiūnas T, Bonde I, Herrgård M, Harrison SJ, Kristensen M, Pedersen LE, Jensen MK, Keasling JD (2015) Multiplex metabolic pathway engineering using CRISPR/Cas9 in *Saccharomyces cerevisiae*. Metab Eng 28:213–222. https://doi.org/10.1016/j.ymben.2015.01.008

Katahira S, Mizuike A, Fukuda H, Kondo A (2006) Ethanol fermentation from lignocellulosic hydrolysate by a recombinant xylose- and cellooligosaccharide-assimilating yeast strain. Appl Microbiol Biotechnol 72:1136–1143. https://doi.org/10.1007/s00253-006-0402-x

Klis FM (1994) Review: cell wall assembly in yeast. Yeast 10(7):851–869. https://doi.org/10.1002/yea.320100702

Lei H, Jin S, Karlsson E, Schultz-Cherry S, Ye K (2016) Yeast surface-displayed H5N1 avian Influenza vaccines. J Immunol Res 2016:4131324–4131312. https://doi.org/10.1155/2016/4131324

Lei H, Xie B, Gao T, Cen Q, Ren Y (2020) Yeast display platform technology to prepare oral vaccine against lethal H7N9 virus challenge in mice. Microb Cell Factories 19(1):53. https://doi.org/10.1186/s12934-020-01316-1

Lesage G, Bussey H (2006) Cell wall assembly in *Saccharomyces cerevisiae*. Microbiol Mol Biol Rev : MMBR 70(2):317–343. https://doi.org/10.1128/MMBR.00038-05

Li B, Scarselli M, Knudsen CD, Kim SK, Jacobson KA, McMillin SM, Wess J (2007) Rapid identification of functionally critical amino acids in a G protein-coupled receptor. Nat Methods 4(2):169–174. https://doi.org/10.1038/nmeth990

Lian J, Schultz C, Cao M, HamediRad M, Zhao H (2019) Multi-functional genome-wide CRISPR system for high throughput genotype-phenotype mapping. Nat Commun 10(1):5794. https://doi.org/10.1038/s41467-019-13621-4

Liu Z, Ho SH, Sasaki K, den Haan R, Inokuma K, Ogino C, van Zyl WH, Hasunuma T, Kondo A (2016) Engineering of a novel cellulose-adherent cellulolytic *Saccharomyces cerevisiae* for cellulosic biofuel production. Sci Rep 6:24550. https://doi.org/10.1038/srep24550

Liu Z, Inokuma K, Ho SH, den Haan R, van Zyl WH, Hasunuma T, Kondo A (2017) Improvement of ethanol production from crystalline cellulose via optimizing cellulase ratios in cellulolytic *Saccharomyces cerevisiae*. Biotechnol Bioeng 114(6):1201–1207. https://doi.org/10.1002/bit.26252

Lu CF, Kurjan J, Lipke PN (1994) A pathway for cell-wall anchorage of *Saccharomyces cerevisiae* alpha-agglutinin. Mol Cell Biol 14(7):4825–4833. https://doi.org/10.1128/mcb.14.7.4825

Moreno-García J, Coi AL, Zara G, García-Martínez T, Mauricio JC, Budroni M (2018) Study of the role of the covalently linked cell wall protein (Ccw14p) and yeast glycoprotein (Ygp1p) within biofilm formation in a flor yeast strain. FEMS Yeast Res 18(2). https://doi.org/10.1093/femsyr/foy005

Moukadiri I, Armero J, Abad A, Sentandreu R, Zueco J (1997) Identification of a mannoprotein present in the inner layer of the cell wall of *Saccharomyces cerevisiae*. J Bacteriol 179(7):2154–2162. https://doi.org/10.1128/jb.179.7.2154-2162.1997

Mrsa V, Ecker M, Strahl-Bolsinger S, Nimtz M, Lehle L, Tanner W (1999) Deletion of new covalently linked cell wall glycoproteins alters the electrophoretic mobility of phosphorylated wall components of *Saccharomyces cerevisiae*. J Bacteriol 181(10):3076–3086. https://doi.org/10.1128/JB.181.10.3076-3086.1999

Nambu-Nishida Y, Nishida K, Hasunuma T, Kondo A (2017) Development of a comprehensive set of tools for genome engineering in a cold- and thermo-tolerant *Kluyveromyces marxianus* yeast strain. Sci Rep 7(1):8993. https://doi.org/10.1038/s41598-017-08356-5

Ragni E, Sipiczki M, Strahl S (2007) Characterization of Ccw12p, a major key player in cell wall stability of *Saccharomyces cerevisiae*. Yeast 24(4):309–319. https://doi.org/10.1002/yea.1465

Ragni E, Piberger H, Neupert C, García-Cantalejo J, Popolo L, Arroyo J, Aebi M, Strahl S (2011) The genetic interaction network of *CCW12*, a *Saccharomyces cerevisiae* gene required for cell wall integrity during budding and formation of mating projections. BMC Genomics 12:107. https://doi.org/10.1186/1471-2164-12-107

Shankarnarayan S, Malone CL, Deschenes RJ, Fassler JS (2008) Modulation of yeast Sln1 kinase activity by the CCW12 cell wall protein. J Biol Chem 283(4):1962–1973. https://doi.org/10.1074/jbc.M706877200

Shibasaki S, Ueda M, Ye K, Shimizu K, Kamasawa N, Osumi M, Tanaka A (2001) Creation of cell surface-engineered yeast that display different fluorescent proteins in response to the glucose concentration.

Appl Microbiol Biotechnol 57(4):528–533. https://doi.org/10.1007/s002530100767

Shibasaki S, Kawabata A, Tanino T, Kondo A, Ueda M, Tanaka M (2009) Evaluation of the biodegradability of polyurethane and its derivatives by using lipase-displaying arming yeast. Biocontrol Sci 14(4):171–175. https://doi.org/10.4265/bio.14.171

Shusta EV, Kieke MC, Parke E, Kranz DM, Wittrup KD (1999) Yeast polypeptide fusion surface display levels predict thermal stability and soluble secretion efficiency. J Mol Biol 292(5):949–956. https://doi.org/10.1006/jmbi.1999.3130

van der Vaart JM, te Biesebeke R, Chapman JW, Toschka HY, Klis FM, Verrips CT (1997) Comparison of cell wall proteins of *Saccharomyces cerevisiae* as anchors for cell surface expression of heterologous proteins. Appl Environ Microbiol 63(2):615–620. https://doi.org/10.1128/aem.63.2.615-620.1997

Wang H, Lang Q, Li L, Liang B, Tang X, Kong L, Mascini M, Liu A (2013) Yeast surface displaying glucose oxidase as whole-cell biocatalyst: construction, characterization, and its electrochemical glucose sensing application. Anal Chem 85(12):6107–6112. https://doi.org/10.1021/ac400979r

Wentz AE, Shusta EV (2007) A novel high-throughput screen reveals yeast genes that increase secretion of heterologous proteins. Appl Environ Microbiol 73(4):1189–1198. https://doi.org/10.1128/AEM.02427-06

Yamakawa S, Yamada R, Tanaka T, Ogino C, Kondo A (2012) Repeated fermentation from raw starch using *Saccharomyces cerevisiae* displaying both glucoamylase and α-amylase. Enzym Microb Technol 50(6-7):343–347. https://doi.org/10.1016/j.enzmictec.2012.03.005

Zhao SX, Guo YH, Wang QN, Luo HL, He CZ, An B (2020) Expression of flagellin at yeast surface increases biocontrol efficiency of yeast cells against postharvest disease of tomato caused by *Botrytis cinerea*. Postharvest Biol Technol 162:111112. https://doi.org/10.1016/j.postharvbio.2019.111112